



Citation for published version:

Belardi, W & Knight, JC 2013, 'Effect of core boundary curvature on the confinement losses of hollow antiresonant fibers', *Optics Express*, vol. 21, no. 19, pp. 21912-21917. <https://doi.org/10.1364/OE.21.021912>

DOI:

[10.1364/OE.21.021912](https://doi.org/10.1364/OE.21.021912)

Publication date:

2013

Document Version

Publisher's PDF, also known as Version of record

[Link to publication](#)

This paper was published in *Optics Express* and is made available as an electronic reprint with the permission of OSA. The paper can be found at the following URL on the OSA website: <http://www.opticsinfobase.org/oe/abstract.cfm?uri=oe-21-19-21912>. Systematic or multiple reproduction or distribution to multiple locations via electronic or other means is prohibited and is subject to penalties under law.

University of Bath

General rights

Copyright and moral rights for the publications made accessible in the public portal are retained by the authors and/or other copyright owners and it is a condition of accessing publications that users recognise and abide by the legal requirements associated with these rights.

Take down policy

If you believe that this document breaches copyright please contact us providing details, and we will remove access to the work immediately and investigate your claim.

Effect of core boundary curvature on the confinement losses of hollow antiresonant fibers

Walter Belardi* and Jonathan C. Knight

Centre for Photonics and Photonic Materials, Department of Physics, University of Bath, Claverton Down, Bath, BA2 7AY, UK
*wb286@bath.ac.uk

Abstract: We use numerical simulations to investigate how the curvature of the fiber core boundary influences the attenuation of hollow antiresonant fibers. We show the importance of a “negative” curvature core boundary in reducing confinement losses and also how, for certain curvatures, optical power is coupled resonantly to cladding modes. We simulate bending losses and find results in agreement with previously-reported experiments.

©2013 Optical Society of America

OCIS codes: (060.2280) Fiber design and fabrication; (060.2400) Fiber properties; (060.4005) Microstructured fibers.

References and links

1. M. A. Duguay, Y. Kokubun, T. L. Koch, and L. Pfeiffer, “Antiresonant reflecting optical waveguides in SiO₂/Si multilayer structures,” *Appl. Phys. Lett.* **49**(1), 13–15 (1986).
2. J. C. Knight, T. A. Birks, P. St. J. Russell, and D. M. Atkin, “All-silica single-mode optical fiber with photonic crystal cladding,” *Opt. Lett.* **21**(19), 1547–1549 (1996).
3. J. C. Knight, J. Broeng, T. A. Birks, and P. S. J. Russell, “Photonic band gap guidance in optical fibers,” *Science* **282**(5393), 1476–1478 (1998).
4. P. St. J. Russell, “Photonic Crystal Fibers,” *Science* **299**(5605), 358–362 (2003).
5. R. F. Cregan, B. J. Mangan, J. C. Knight, T. A. Birks, P. St. J. Russell, P. J. Roberts, and D. C. Allan, “Single-mode photonic band gap guidance of light in air,” *Science* **285**(5433), 1537–1539 (1999).
6. F. Benabid, J. C. Knight, G. Antonopoulos, and P. St. J. Russell, “Stimulated Raman scattering in hydrogen-filled hollow-core photonic crystal fiber,” *Science* **298**(5592), 399–402 (2002).
7. A. Argyros, S. G. Leon-Saval, J. Pla, and A. Docherty, “Antiresonant reflection and inhibited coupling in hollow-core square lattice optical fibres,” *Opt. Express* **16**(8), 5642–5648 (2008), <http://www.opticsinfobase.org/oe/abstract.cfm?URI=oe-16-8-5642>.
8. S. Février, B. Beaudou, and P. Viale, “Understanding origin of loss in large pitch hollow-core photonic crystal fibers and their design simplification,” *Opt. Express* **18**(5), 5142–5150 (2010), <http://www.opticsinfobase.org/oe/abstract.cfm?URI=oe-18-5-5142>.
9. F. Gérôme, R. Jamier, J. L. Auguste, G. Humbert, and J. M. Blondy, “Simplified hollow-core photonic crystal fiber,” *Opt. Lett.* **35**(8), 1157–1159 (2010).
10. A. D. Pryamikov, A. S. Biriukov, A. F. Kosolapov, V. G. Plotnichenko, S. L. Semjonov, and E. M. Dianov, “Demonstration of a waveguide regime for a silica hollow-core microstructured optical fiber with a negative curvature of the core boundary in the spectral region $> 3.5 \mu\text{m}$,” *Opt. Express* **19**(2), 1441–1448 (2011), <http://www.opticsinfobase.org/oe/abstract.cfm?URI=oe-19-2-1441>.
11. F. Benabid, P. J. Roberts, F. Couny, and P. S. Light, “Light and gas confinement in hollow-core photonic crystal fibre based photonic microcells,” *J. Eur. Opt. Soc. Rapid Publ.* **4**, 09004 (2009), https://www.jeos.org/index.php/jeos_rp/article/view/09004.
12. J. Anthony, R. Leonhardt, S. G. Leon-Saval, and A. Argyros, “THz propagation in kagome hollow-core microstructured fibers,” *Opt. Express* **19**(19), 18470–18478 (2011), <http://www.opticsinfobase.org/oe/abstract.cfm?URI=oe-19-19-18470>.
13. A. Urlich, R. R. J. Maier, F. Yu, J. C. Knight, D. P. Hand, and J. D. Shephard, “Flexible delivery of Er:YAG radiation at $2.94 \mu\text{m}$ with negative curvature silica glass fibers: a new solution for minimally invasive surgical procedures,” *Biomed. Opt. Express* **4**(2), 193–205 (2013).
14. Y. Y. Wang, N. V. Wheeler, F. Couny, P. J. Roberts, and F. Benabid, “Low loss broadband transmission in hypocycloid-core Kagome hollow-core photonic crystal fiber,” *Opt. Lett.* **36**(5), 669–671 (2011).
15. A. F. Kosolapov, A. D. Pryamikov, A. S. Biriukov, V. S. Shiryaev, M. S. Astapovich, G. E. Snopatin, V. G. Plotnichenko, M. F. Churbanov, and E. M. Dianov, “Demonstration of CO₂-laser power delivery through chalcogenide-glass fiber with negative-curvature hollow core,” *Opt. Express* **19**(25), 25723–25728 (2011), <http://www.opticsinfobase.org/oe/abstract.cfm?URI=oe-19-25-25723>.
16. F. Yu, W. J. Wadsworth, and J. C. Knight, “Low loss silica hollow core fibers for 3–4 μm spectral region,” *Opt. Express* **20**(10), 11153–11158 (2012), <http://www.opticsinfobase.org/oe/abstract.cfm?URI=oe-20-10-11153>.

17. F. Yu and J. C. Knight, "Limits of hollow core negative curvature fiber," in Proceedings of CLEO 2013, paper CTu2K6.
 18. F. Poletti, J. R. Hayes, and D. J. Richardson, "Optimising the performances of hollow antiresonant fibres," in Proceedings of ECOC 2011, paper Mo.2.LeCervin.2.
 19. J. Olszewski, M. Szpulak, and W. Urbańczyk, "Effect of coupling between fundamental and cladding modes on bending losses in photonic crystal fibers," *Opt. Express* **13**(16), 6015–6022 (2005), <http://www.opticsinfobase.org/oe/abstract.cfm?URI=oe-13-16-6015&origin=search>.
 20. K. Saitoh, N. Mortensen, and M. Koshiba, "Air-core photonic band-gap fibers: the impact of surface modes," *Opt. Express* **12**(3), 394–400 (2004), <http://www.opticsinfobase.org/oe/abstract.cfm?URI=oe-12-3-394>
-

1. Introduction

Antiresonance has long been known [1] as a mechanism enabling light confinement to a medium with a refractive index lower than that of its surroundings. However the mechanism has received increased attention in fiber optics following the discovery and development of Photonic Crystal Fibers (PCFs) [2–4]. While seeking efficient light guidance in hollow core PCFs [5], a novel type of fiber was developed by arranging its cladding holes in a Kagomé lattice [6]. This fiber guided light by means of an antiresonant effect and allowed for a much broader spectral transmission than that achieved in photonic bandgap fibers [3, 4].

Hollow core antiresonant fibers (ARFs) have been studied [7] and several attempts have been made to simplify their geometrical structure [8–10]. The realization of ARFs with an extended transmission window and low losses could have a wide range of applications ranging from gas-light interaction [11] to terahertz applications [12] and medicine [13].

Recently it has been shown that the curvature of the core boundary of ARFs may significantly affect their losses [10, 14]. In ref. 14 the authors reported on a hypocycloid-core Kagomé ARF with a minimum loss of 130dB/km at 1.317 μm . They explained that the reduction of 1 order of magnitude in the confinement losses of this fiber (compared to the one in ref. 6) was related to the modification of the fiber core boundary shape. According to them, a change in the core boundary shape may reduce the overlap between the core modes and the cladding modes of the fiber, by having the effect of an overall reduction of the fiber losses. The authors estimated that this power coupling between core and cladding modes could be reduced by increasing the length of the silica webs surrounding the fiber core or by reducing their thickness [14]. Thus they speculated that the elongation of the silica webs in the hypocycloid-core Kagome ARF [14] compared to the circular-core Kagome ARF [6] was responsible for the loss reduction.

In ref. 10 the authors provided a different explanation for the reduction of confinement losses in ARFs with a simplified structure. They introduced the word "negative curvature" by referring to the fact that the core boundary has a convex shape when seen from the center of the fiber. They claimed that a "negative curvature" of the core boundary was responsible for loss reduction of ARFs in the near and medium infrared regime [10, 15]. They argued that the presence of a "negative curvature" was effective in reducing the spatial overlap between the core mode and the silica core boundary, therefore minimizing the overall fiber losses.

Negative Curvature Fibers (NCFs) have recently been demonstrated with losses as low as 34dB/km at 3.05 μm [16] and 24dB/km at 2.4microns [17]. Further improvement in their performance will rely on better understanding the relationship between the core boundary curvature and the confinement losses.

In this work we provide a detailed numerical analysis of the relationship between the core boundary curvature and the confinement losses in ARFs, and show the importance of the "negative curvature" for reducing loss. We show that this relationship can be affected by resonant coupling between core and cladding modes. We also validate some previous experimental observations on bending losses.

2. Negative curvature fiber

We used the commercially available finite-element software Comsol to perform our numerical analysis. We first validated our model through comparison with Refs. [18–20], and by performing convergence tests. We then based our fiber design on the structure and

geometrical parameters of an NCF previously reported [16]. A section of the modelled fiber is shown in Fig. 1. The core radius r_c is $47\mu\text{m}$, the thickness of the silica struts and of the core wall t is $2.66\mu\text{m}$ and the inner radius of the silica cladding tube is $OA = 128.75\mu\text{m}$. Since the fiber in ref. 16 has a minimum loss at the wavelength of $3.05\mu\text{m}$, we have decided to adopt this wavelength for our numerical analysis. However the losses of silica material have not been included in our model.

2.1 Design

The design method used for studying the relation between the confinement losses and the core boundary curvature is shown in Fig. 1. While calculating the confinement losses, the fiber core radius is kept constant at a value $r_c = 47\mu\text{m}$ and the contact point between adjacent cladding holes C is moving along the straight line OA . The core boundary is then built by connecting the moving point C to the fixed point R with an arc whose circle has center in P and radius r_s . In this way, the modification of the fiber geometry allows us to evaluate several different fiber structures with the same core radius r_c , core wall thickness t and cladding tube radius OA but different curvatures of the core boundary $Curv = 1/r_s$. As shown on the right hand side of Fig. 1, the fiber structure passes from structure “a” with a very low curvature of the core boundary to structure “c” where the core boundary curvature reaches its maximum value.

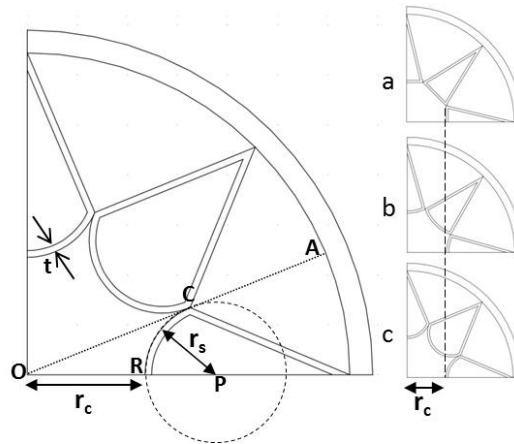


Fig. 1. Design of a negative curvature fiber: modification of the NCF geometry is obtained by moving the point C along the straight line OA . In this way the fiber structure passes from “a” to “c,” as shown on the left hand side. The fiber core radius is kept fixed at $47\mu\text{m}$.

2.2 Numerical results

Figure 2 shows the numerical results obtained. The confinement losses (blue line with dots) shown on the left axis are evaluated for different values of the core boundary curvature $Curv$ which varies from 525m^{-1} to a maximum value $Curv_{MAX} = 34322\text{m}^{-1}$ (when the lines meeting at C are parallel), corresponding to a curvature radius $r_{sMAX} = 29.14\mu\text{m}$. The “normalized curvature” is obtained by dividing each curvature by the maximum value $Curv_{MAX}$. The right hand axis (red line with triangles) indicates the values of the effective mode area of the NCF. A magnification of the plot is shown on the right hand side, for values of the normalized curvature between 0.9 and 1.

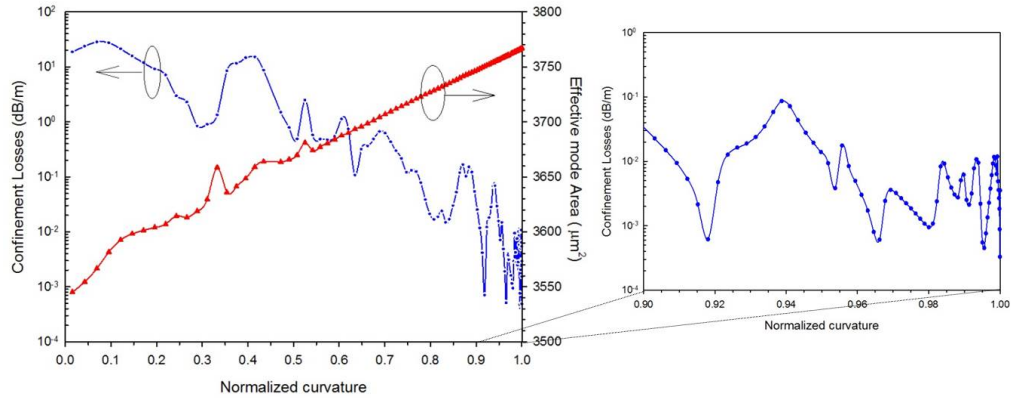


Fig. 2. Relationship between confinement losses (blue line with dots, left axis) and normalized curvature of a NCF. The values of the effective mode area of the NCF (red line with triangles) are indicated on the right axis. On the right hand side is a magnification of the same plot for values of the normalized curvature between 0.9 and 1.

The plot shows that the confinement losses can be reduced by around 4 orders of magnitude by adopting high curvature. The reduction is not monotonic, with several peaks appearing in the curve. As a side effect of the increased “negative” curvature, the effective mode area of the fundamental mode increases by 6% in a roughly linear way. Its value passes from $3545 \mu\text{m}^2$ to $3767 \mu\text{m}^2$. It should be noted that for other nearby wavelengths, although the details of the curves will differ, the overall trend remains the same.

We have also calculated the percentage of optical power in the hollow core, in all the air holes and in the silica cladding of the fiber. The results are shown in Fig. 3.

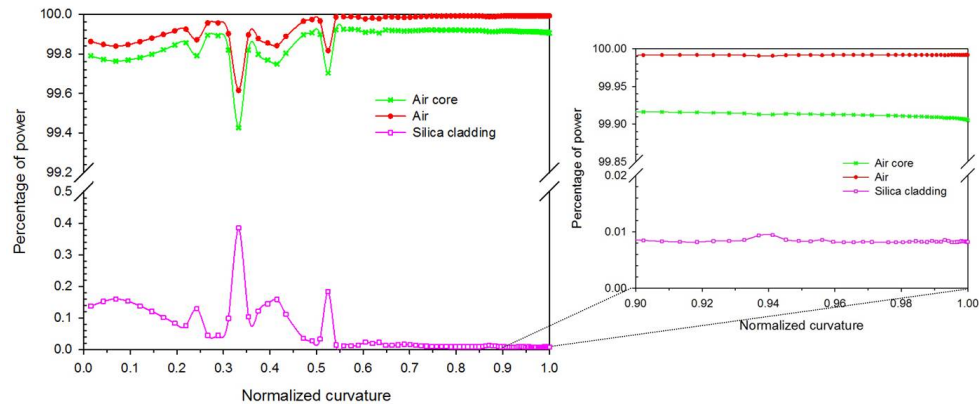


Fig. 3. Percentage of optical power in the air core (green line with ‘x’), in all the air holes of the fiber (red line with filled dots) and in the silica struts of the cladding (purple line with empty dots). On the right hand side is a magnification of the plot for curvature values between 0.9 and 1.

The percentage of optical power in the hollow core of the NCF reaches a maximum value of about 99.9% when the normalized curvature is close to 1. The optical power in the silica struts of the cladding decreases to less than 0.01%, consistent with the absorptive loss measurements reported in ref. 17. About 0.09% of the optical power is found in the cladding air holes. The peaks in the silica cladding curve in Fig. 3 are linked to the peaks in the confinement losses observed in Fig. 2.

2.3 Coupling effect

In order to explain the origin of the local peak losses observed in Fig. 2, we have analyzed a specific normalized curvature range around the value of 0.521 (see Figs. 2 and 3), corresponding to one of the peaks. The results are shown in Fig. 4.

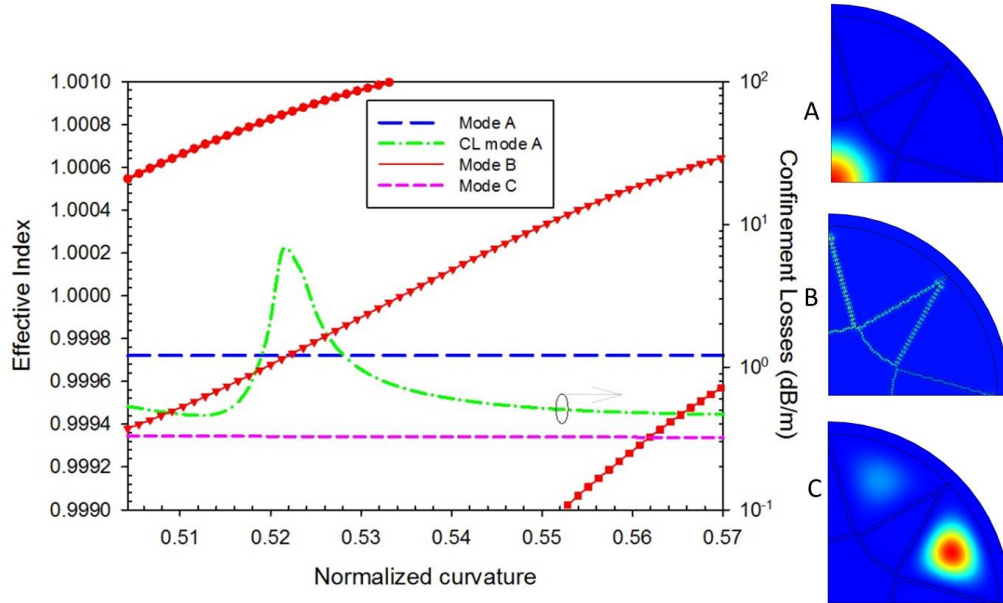


Fig. 4. The air core mode (blue - A) and a silica cladding mode (red - B) cross at the value of the curvature corresponding to the loss peak in the confinement loss curve (shown in green). Poynting vector plots are shown on the right: C is a low-dispersion (air) cladding mode.

We have calculated the effective index of all optical modes present in the fiber in the range 0.999-1.001. These modes belong to three categories which are shown on the right side of Fig. 4: the degenerate fundamental-like core mode (A), silica cladding modes (B) and degenerate air hole cladding modes (C). Figure 4 shows the evolution of the effective index with the curvature for modes A (blue long-dashed line), B (red lines with circles, triangles and squares) and C (purple short-dashed line). The peak in confinement loss of the core mode (green dashed-dotted line) corresponds to the crossing between modes A and B. We conclude that the loss peak is caused by the strong coupling between modes A and B at the specific normalized curvature of 0.521. It should be noted that the same behavior has been observed also for other peak losses of Fig. 2 at low as well as at high curvature, which leads us to generalize this result to all peak losses. We should also clarify that this “local” longitudinal phase matching does not explain the overall trend of reduced confinement loss with curvature observed in Fig. 2. This has been explained in ref. 14 as related to an overall diminished power coupling between the air core mode and the rapidly-oscillating transverse field of the silica-confined cladding mode.

2.4 Importance of the negative curvature

For the sake of completeness, we report here that we have also performed numerical simulations on an identical structure to that shown in Fig. 1 but applying a “positive” curvature to the core boundary. In this case, the arc used to build the core boundary belongs to a circle whose center is not in the cladding area (as in Fig. 1) but in the core. The core boundary then presents a concave shape when seen from the center of the fiber. By using this design, we could compare the performances of two different fiber types with exactly the same parameters (and similar elongations of the silica webs surrounding the core) but opposite curvatures of the core boundary (“negative” or “positive”). In this case the confinement losses

were never lower than a few dB/m, proving that the positive curvature was not effective in reducing the mode overlap between fundamental and cladding modes. We conclude that the “negative” curvature of the core boundary is essential for reducing confinement losses.

2.5 Bending losses

We have adopted the method of ref. 19 to simulate propagation in a bent NCF with a maximum curvature $Curv_{MAX} = 34322\text{m}^{-1}$ (normalized curvature of 1). The bending direction that has been chosen is the one along the x-axis. We have first analyzed the relationship between confinement losses and bend radius at the wavelength of $3.05\ \mu\text{m}$ (left hand side of Fig. 5). As in Fig. 2, this relationship is affected by the evolution of the coupling between air-core and cladding modes, which is particularly visible in the two loss peaks at the bend radii $R_b = 7\text{cm}$ and $R_b = 17\text{cm}$. On the right hand side of Fig. 5, we have shown the confinement losses of the bent NCF across its full transmission window for different bend radii R . Overall, bend losses are lower on the longer-wavelength side of the transmission window. By comparing the curve with $R = 5\text{cm}$ (dark blue line with dots) and that one with $R = 15\text{cm}$ (green line with diamonds), we can see that the wavelength of the loss peaks change. As a consequence of this wavelength shift, if we consider the wavelength range around $3.2\ \mu\text{m}$, the confinement losses of the NCF are greater for a bend radius $R = 15\text{cm}$ (green line with diamonds) than for a smaller bend radius $R = 10\text{cm}$ (red line with “x”). A very similar behavior was already observed experimentally in Fig. 4 of ref. 13.

Finally, the confinement losses of the considered NCF are only marginally affected by the bending when the bend radius is greater than about 20cm , as also shown experimentally in ref. 13.

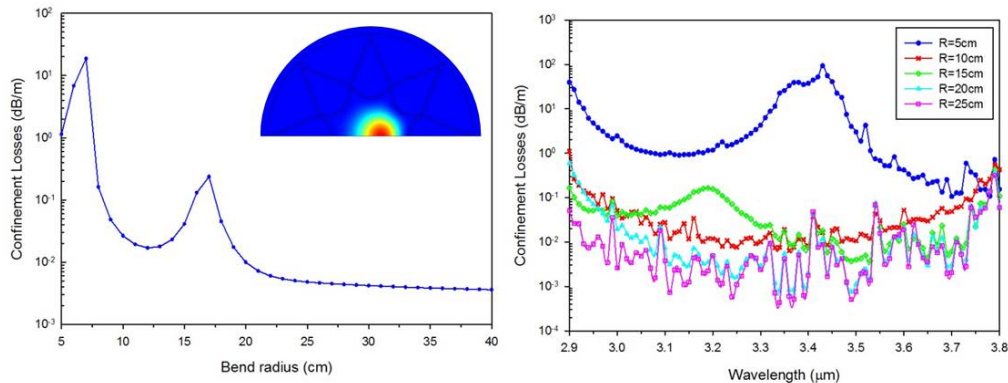


Fig. 5. The relationship between confinement losses and bend radius is strongly affected by the coupling between air-core and cladding modes, which causes some peak losses. The wavelength associated to these peaks also depends on the particular bend radius adopted.

3. Conclusion

We have studied the impact of the core boundary curvature on the confinement losses of hollow antiresonant fibers designed with similar geometrical characteristics to those previously reported. We have identified the origin of the observed loss peaks in the coupling between the air-core and cladding modes of the fiber. We have outlined the importance of a “negative” curvature core boundary for achieving loss reduction and studied the specific evolution of the fiber bending losses.

Acknowledgements

The authors would like to thank Tim Birks, Fei Yu and William Wadsworth for useful discussions. This work was funded by the UK Engineering and Physical Sciences Council under EP/I011315/1.